

# Connecting polymers to the quantum Hall plateau transition

Joel E. Moore

*Bell Labs Lucent Technologies, 600 Mountain Avenue, Murray Hill, NJ 07974*

(November 20, 2018)

A mapping is developed between the quantum Hall plateau transition and two-dimensional self-interacting lattice polymers. This mapping is exact in the classical percolation limit of the plateau transition, and diffusive behavior at the critical energy is shown to be related to the critical exponents of a class of chiral polymers at the  $\theta$ -point. The exact critical exponents of the chiral polymer model on the honeycomb lattice are found, verifying that this model is in the same universality class as a previously solved model of polymers on the Manhattan lattice. The mapping is obtained by averaging analytically over the local random potentials in a previously studied lattice model for the classical plateau transition. This average generates a weight on chiral polymers associated with the classical localization length exponent  $\nu = 4/3$ . We discuss the differences between the classical and quantum transitions in the context of polymer models and use numerical results on higher-moment scaling laws at the quantum transition to constrain possible polymer descriptions. Some properties of the polymer models are verified by transfer matrix and Monte Carlo studies.

PACS numbers: 73.43.Nq, 72.15.Rn, 61.41.+e

## I. INTRODUCTION

The quantum Hall plateau transition is of great interest because it links Anderson localization and the quantum Hall effect (QHE), two of the fundamental phenomena of condensed matter physics. Noninteracting electrons moving in two dimensions in a random potential form energy eigenstates which do not extend to infinity but are exponentially localized in finite regions of the plane. The situation changes drastically in a magnetic field: there are then extended states at discrete critical energies  $E_c$  separated by the cyclotron energy  $\hbar\omega_c$ . These extended states are remnants of the Landau bands at zero disorder. At other energies the electron eigenstates are localized, and the localization length near a critical energy scales according to

$$\xi(E) = \xi_0 \left( \frac{E_c}{E - E_c} \right)^\nu. \quad (1.1)$$

An understanding of this behavior, which determines the passage from one quantum Hall plateau to another, is essential to the explanation of the integer QHE<sup>1</sup>. Despite progress in finding an effective theory for this transition<sup>2,3</sup>, the scaling law (1.1) and other universal properties of the transition have still not been obtained analytically.

The clearest picture for the scaling (1.1) remains the connection between hulls of percolation clusters and classical electron trajectories in a strong magnetic field and random potential<sup>4</sup>. Classical percolation was recently shown to describe correctly some aspects of the *spin* quantum Hall transition<sup>5</sup>, but the ordinary quantum Hall transition is known from numerical studies<sup>6,7</sup> not to lie in the percolation universality class. Considerable effort has been devoted to how quantum effects modify the percolation picture, and while there is now an understanding via numerics of the essential ingredients required to

model the transition<sup>7</sup>, analytic progress on generalizing percolation has been quite limited<sup>8</sup>. This paper develops a mapping between the plateau transition and the physics of self-interacting two-dimensional lattice polymers. Many statistical properties are known for such polymers because they in turn can be mapped to simple magnetic systems with known critical properties<sup>9,10</sup>. The final section discusses how quantum effects might be incorporated in a polymer description. However, numerically determined scaling laws for higher moments in the quantum case, which result from strong interference of quantum paths, seem to rule out a simple polymer mapping.

The properties of a lattice version of the classical plateau transition are mapped after disorder averaging onto polymers at the  $\theta$ -point, which is a tricritical point separating the collapsed and extended phases of polymers with an attractive short-ranged self-interaction. The polymer model for the classical transition gives a useful complementary picture to the percolation description, in which some facts, such as diffusion at the critical energy, are more easily recovered. A side benefit is that some new results on polymers come out naturally from the mapping to the plateau transition.

The polymer mapping provides an alternate connection between the classical limit of the plateau transition and (classical) percolation<sup>4,11,12</sup>, as ring polymers at the  $\theta$ -point are equivalent to percolation hulls<sup>13,14</sup>. One result of this paper is that directly mapping the plateau transition to polymers without the intermediate step of percolation gives many more relations. The exponent  $\nu_\theta$  which governs the typical size of a polymer (for a polymer of  $N$  units,  $\langle R^2 \rangle \sim N^{2\nu_\theta}$ , where  $\langle \rangle$  denote averages over the ensemble of polymers), and  $\mu$  and  $\gamma$  which determine essentially the number  $\sim \mu^N N^{\gamma-1}$  of polymers of length  $N$ , can all be connected to the plateau transition.

The localization length exponent in (1.1) is  $\nu = \frac{4}{3}$  for

classical percolation, while numerical studies<sup>6,7</sup> for the quantum case predict  $\nu = 2.35 \pm 0.05$  for the lowest Landau level (LLL), consistent with experiments<sup>15</sup>. In this paper  $\nu$  will be studied via the subdiffusive propagation of electrons in a magnetic field and quenched random potential, which is now reviewed. Recently it was shown by Sinova, Meden, and Girvin<sup>16</sup> that the localization length exponent  $\nu$  appears in the energy-integrated correlation function  $\Pi(x, t) \equiv \langle\langle \bar{\rho}(0, 0) \bar{\rho}(x, t) \rangle\rangle$ , where  $\bar{\rho}$  is the LLL-projected electron density operator and  $\langle\langle \rangle\rangle$  denote disorder averaging. (The discussion in this paper is generally restricted to the LLL, although  $\nu$  is believed to be universal.) The Fourier transform was verified numerically to have the scaling form

$$\omega \text{Im}\Pi(q, \omega) = \omega^{\frac{1}{2\nu}} f(q^2/\omega) \quad (1.2)$$

in the limit  $q, \omega \rightarrow 0$  with  $q^2 \ll \omega$ . This scaling form can be understood as resulting from a simple form for  $\Pi(q, \omega)$  in this limit,

$$\Pi(q, \omega) \sim \frac{1}{\omega - iD(\omega)q^2}, \quad (1.3)$$

with the frequency-dependent diffusion constant  $D(\omega) \propto \omega^{\frac{1}{2\nu}}$ .

The result (1.2) depends on the assumption that only at isolated critical energies  $E_c$  are there extended states. It can be understood from the following argument, which is somewhat different from that in<sup>16</sup>. Electrons at energy  $E$  with localization length  $\xi(E)$  move diffusively over short times but cross over to localized behavior once  $t \geq \xi(E)^2/D_0$ . The diffusion constant  $D_0$  should have a finite limit as  $E \rightarrow E_c$  since the conductivity  $\sigma_{xx}$  is finite at the transition, and can be approximated by this limiting value in the scaling limit. So for a particle at the origin at  $t = 0$  (where it projects onto eigenstates of different energies),

$$\langle x^2(t) \rangle \approx \int_{\xi(E)=\sqrt{D_0 t}}^{\infty} dE \rho \xi^2(E) + \int_{E_c}^{\xi(E)=\sqrt{D_0 t}} dE \rho D_0 t. \quad (1.4)$$

where  $\rho$  is the density of states near  $E_c$ . This results in subdiffusive behavior:

$$\tilde{D} \equiv \frac{d}{dt} \langle x^2(t) \rangle = \rho E_c D_0 \left( \frac{\xi_0}{\sqrt{D_0}} \right)^{\frac{1}{\nu}} t^{-\frac{1}{2\nu}}, \quad (1.5)$$

which corresponds to (1.2) with  $f(x) \propto x$  for  $x \ll 1$ .

Our starting point to obtain the anomalous diffusion (1.2) is a single electron moving either classically or quantum-mechanically in the  $x$ - $y$  plane in a random potential  $V(x)$  and strong constant magnetic field  $B\hat{z}$ . The classical coarse-grained equation of motion

$$B\dot{\mathbf{x}}_i = -\epsilon_{ij} \partial_j V(x) \quad (1.6)$$

can also be obtained<sup>12</sup> by taking a certain limit of the Liouvilian formalism. The lowest-Landau-level projected electron density operator in this limit becomes a classical distribution function of particles moving according to (1.6). Of course, the equation of motion (1.6) can also be derived simply from classical physics: a single electron moving in constant electric and magnetic fields with  $E < B$  has average velocity  $\frac{E}{B}c$  along the direction  $\mathbf{E} \times \mathbf{B}$ . Since the direction of motion is always perpendicular to  $\nabla V$ , the particle moves along a constant-energy contour of the potential. The picture underlying network models<sup>7</sup> of the transition is that electron propagation is nearly classical except near a saddle point of the potential, where quantum tunneling becomes significant.

The first part of this paper shows that a discrete-time lattice version of (1.6), known to have the correct (percolative) critical scaling for the classical limit, maps after disorder averaging onto a model of two-dimensional interacting polymers on the same lattice. Although the lattice is useful to derive the mapping, the critical properties related by the mapping are universal and hence lattice-independent. In the remainder of the introduction, we outline the lattice model of (1.6) and some basic properties of interacting polymers, then summarize the main results.

In order to establish the connection between polymers and motion along level surfaces, we use a lattice model due to Gurarie and Zee<sup>12</sup>. The particle is taken to have constant velocity along level surfaces: a nonzero mean velocity at criticality was found numerically in<sup>11,12</sup> for similar models, and fixing the particle velocity does not alter the critical scaling. Particles move on the edges of the honeycomb lattice of Fig. 1, where each hexagonal face has an associated random potential energy. Except in section II, the energy  $E$  of a particle starting at vertex  $A$  will be taken to be the average of the three neighboring potentials  $V_1, V_2, V_3$ , instead of an independent quantity as in<sup>12</sup>. The energy  $E$  is constant along the particle trajectory. The particle's first step is chosen so that the potential to the left is larger than the particle energy  $E$ , which is larger than the potential to the right. In successive steps, there is always a choice between two directions aside from the direction by which the particle entered, and only one of these choices will satisfy the condition that the energy to the left (right) be greater (less) than  $E$ . For each realization of the random potentials and each starting point, there is a unique locus of the particle after  $N$  steps. The connection to the classical localization exponent  $\nu = \frac{4}{3}$  is that the mean square displacement after  $N$  steps is found to show subdiffusive behavior:

$$\langle\langle R^2(N) \rangle\rangle \sim N^{1-\frac{1}{2\nu}} \quad (1.7)$$

in accord with (1.5). The value  $1 - \frac{1}{2\nu} \approx 0.62$  was found by numerical simulation<sup>12</sup> of (1.6), compared to the predicted value  $\frac{5}{8} = 0.625$ .

Now the connection between motion along level surfaces (1.6) and percolation hulls is quickly reviewed. Con-

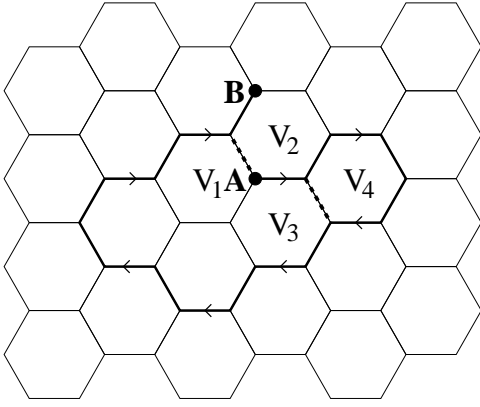


FIG. 1. Sample self-avoiding walk from  $A$  to  $B$  of 20 steps, with 19 neighboring hexagons. The dotted edges are self-contacts: the edge between  $V_3$  and  $V_4$  is an antiparallel self-contact, while that between  $V_1$  and  $V_2$  is a parallel self-contact. This path is not allowed classically since the walk passes  $V_2$  both on the left and on the right.

consider the level-surface motion on the hexagonal lattice with white-noise potentials (i.e., the disorder correlation length  $\lambda_D$  is less than the lattice spacing). Then all potentials on the left of a trajectory are higher than the trajectory energy  $E$ , which is higher than all potentials on the right. Now let all faces with energy higher than  $E$  be “colored”, while those with energy lower than  $E$  remain uncolored. The trajectory is then a hull separating colored faces from uncolored ones, and the properties of such hulls are a standard problem in percolation. Although the choice of lattice affects such properties as the density of colored faces at the critical point, critical exponents are universal (independent of the lattice). Similarly a lattice model is used here to establish the mapping to a polymer problem, but the universal polymer properties  $\gamma$  and  $\nu$  discussed below do not depend on this lattice.

The usual way to study this type of lattice model<sup>11,12</sup> is by summing numerically over paths at fixed particle energy. Here the path will be held fixed for the integration over random potentials: the goal is to assign a weight to each path according to the fraction of the space of random potentials for which that path is the particle trajectory. For convenience, the potentials are assumed to be uniformly distributed on  $[-1, 1]$ , so the critical energy is  $E_0 = 0$ . After  $N$  steps the particle has either moved along a self-avoiding walk (SAW) of length  $N$ , or else has looped and begun retracing previous steps. There is a constraint of “no parallel self-contacts” (the terminology is explained in section II) on allowed SAWs resulting from the restriction that no hexagon can be passed on both the left and right (Fig. 1).

The probability  $P(a, b, N)$  to reach  $b$  from  $a$  after  $N$  steps can be written as a sum over an ensemble of paths including both closed self-avoiding polygons (SAPs) as well as open SAWs with no parallel self-contacts. Writing  $W^i$  for the weight of closed or open curve  $i$ , the disorder-

averaged probability to be at  $b$  after  $N$  steps starting from  $a$  is ( $H$  is the number of different hexagons visited by the SAW or SAP)

$$P(a, b, N) \propto \sum_{\substack{\text{SAPs } i \text{ through } a \text{ and } b, \\ l = \text{length of SAP}, \\ q = \text{steps from } a \text{ to } b}} \delta_{N \bmod l, q} W^i + \sum_{\substack{\text{SAWs } j \text{ of length } N \\ \text{from } a \text{ to } b \\ \text{no } \parallel \text{ self-contacts}}} W^j. \quad (1.8)$$

In the above each SAP should actually be summed twice, once with distance  $q$  and once with distance  $l - q$ . The  $\delta$ -function in the SAW part ensures that the particle location after  $N$  steps is  $b$ . Sections II and III carry out the disorder average to calculate the weights  $W^{i,j}$  exactly for cases of interest. The weights turn out to have a natural interpretation in terms of self-interacting polymers.

In section II we demonstrate that the trajectories of the lattice model at the critical energy  $E$  are related to a chiral polymer model, whose exact critical properties are found. The property of diffusion at the critical energy is shown to follow from the critical exponents  $\gamma = \frac{6}{7}$  and  $\nu_\theta = \frac{4}{7}$  of the polymer problem. Then in section III we modify the model so that the energy of a trajectory is a function of initial position rather than an independent quantity, and study the localization exponent  $\nu$ . An inequality is derived which connects  $\nu$  to the exponents of the associated polymer problem. Finally, in section IV we discuss modifications resulting from quantum-mechanical effects, which are most clearly apparent in scaling laws for higher moments of the particle distribution function.

## II. TRAJECTORIES AT THE CRITICAL ENERGY

At the critical energy, the particle motion is diffusive:  $\langle\langle R^2(N) \rangle\rangle \sim N$  for long times  $N$ . This section shows that the conditional probability  $P(a, b, N, E_0)$  for the particle moves from  $a$  to  $b$  after  $N$  steps, given that the particle energy is the critical energy  $E_0$ , is related to critical properties of self-interacting polymers at the  $\theta$ -point. Then in the following section the same mapping will be shown to give information about trajectories at other energies, and hence about  $\nu$ . We note in passing that in the percolation picture, diffusion at the critical energy is somewhat surprising. A particle on the hull of the infinite cluster moves superdiffusively, while a particle on a finite cluster has only bounded motion: the diffusive motion obtained after averaging over initial position essentially interpolates between these two limits.

For a path  $P_{AB}$  at the critical energy  $E_0$ , the probability that  $P_{AB}$  is the trajectory in a random potential realization is proportional to  $2^{-H_L} 2^{-H_R} = 2^{-H}$ . Here  $H_L$  ( $H_R$ ) is the number of hexagons passed on the left (right) by the path, and  $H = H_L + H_R$ : the probability

$2^{-H}$  comes about because each hexagon  $i$  with potential  $V_i$  is as likely to have  $V_i > E_0$  as to have  $V_i < E_0$ . Then the ensemble (1.8) becomes

$$P(a, b, N, E_0) = \sum_{\substack{\text{SAPs through } a \text{ and } b, \\ l = \text{length of SAP}, \\ q = \text{steps from } a \text{ to } b}} \frac{\delta_{N \bmod l, q}}{2^H} + \sum_{\substack{\text{SAWs of length } N \\ \text{from } a \text{ to } b \\ \text{no } \parallel \text{ self-contacts}}} \frac{1}{2^H}. \quad (2.1)$$

The connection to self-interacting polymers appears because the number of hexagons visited by an SAW is related to the number of self-contacts of the SAW. A self-contact is a point where the SAW is within one edge of intersecting itself. Counting hexagons in lieu of self-contacts gives rise to the famous  $\theta'$  model<sup>13,14</sup> of a two-dimensional self-interacting polymer. The number of hexagons visited by an SAW of length  $N$  is  $H = N + 1 - N_2 - 2N_3$ , where  $N_2$  and  $N_3$  are the numbers of hexagons visited twice and thrice by the SAW. Checking possible paths on the lattice shows that  $H = N + 1 - I - I'$ , where  $I$  is the number of self-contacts and  $I'$  the number of a certain type of next-nearest-neighbor contacts. The effects of  $I'$  are not believed to alter the universality class of the model<sup>13,14</sup> and will be ignored. The weight  $2^{-H} = 2^{-N-1+I}$  thus corresponds to the grand-canonical ensemble for polymers at chemical potential  $\mu = -\log 2$  and with an attractive interaction energy  $\beta U = -\log 2$  for each self-contact. We call a self-contact parallel (antiparallel) if, once a direction is defined along the polymer, the two sections of polymer in contact have the same (opposite) direction. For a long polymer, almost all self-contacts are antiparallel, as might be expected since parallel self-contacts are a boundary effect, in the weak sense that a closed polymer has none.

There are three phases of the  $\theta'$  model for a two-dimensional self-interacting polymer. At high temperature, the statistical properties are those of the non-interacting SAW, and the mean radius of gyration is  $R \sim N^{3/4}$ . At low temperature, the polymer is in a collapsed phase with  $R \sim N^{1/2}$ . There is a tricritical point, called the  $\theta$ -point, separating these two behaviors, with  $R \sim N^{4/7}$ . The importance of the  $\theta$ -point for the plateau transition is that the weight  $2^{-H}$  corresponds exactly to the  $\theta$ -point on a honeycomb lattice. The chirality constraint will be shown to change the scaling and give the same universal properties as the solvable Manhattan lattice  $\theta$ -point.

Now the diffusion at the critical energy can be obtained from (1.8). Considering for the moment only the SAW term in (1.8), the mean particle displacement after  $N$  steps is

$$\langle\langle R^2(N) \rangle\rangle = \sum_b P(a, b, N) (\mathbf{x}_b - \mathbf{x}_a)^2$$

$$= \sum_{\text{SAWs of length } N} \frac{R_{\text{SAW}}^2}{2^H} \sim \mu^N N^{\gamma-1+2\nu_\theta}. \quad (2.2)$$

Here we have introduced the standard polymer exponents  $\gamma$  and  $\nu_\theta$ , defined through

$$\sum_{\text{SAWs of length } N} \frac{1}{2^H} \sim \mu^N N^{\gamma-1} \\ \frac{\sum_{\text{SAWs of length } N} \frac{R_{\text{SAW}}^2}{2^H}}{\sum_{\text{SAWs of length } N} \frac{1}{2^H}} \sim N^{2\nu_\theta}. \quad (2.3)$$

For ordinary polymers (no chirality constraint) at  $\theta$ ,  $\mu = 1$ ,  $\gamma = \frac{8}{7}$ , and  $\nu_\theta = \frac{4}{7}$ . The effect of the chirality constraint is clearly to reduce  $\gamma$ , since some polymers are forbidden: in fact we now show that  $\gamma = \frac{6}{7}$  with the chirality constraint ( $\mu$  and  $\nu_\theta$  are unchanged), so that  $\langle\langle R^2(N) \rangle\rangle \propto N$  in (2.2) and motion is diffusive at the critical energy.

The critical properties of chiral polymers at  $\theta$  are actually related in a very simple way to those of ordinary polymers at  $\theta$ . As shown at the end of this section, the transfer matrix for  $L$  chiral polymers on a cylinder of finite circumference  $N$  hexagons has the same leading eigenvalue as the transfer matrix of  $2L$  nonchiral polymers on the same cylinder. This means that the critical exponents for the chiral model can be deduced from the known values for the nonchiral model.

The “watermelon” exponents  $x_L$ <sup>10,14</sup> are defined from the correlation functions  $G_{n,L}(a, b)$  of  $L$  mutually avoiding SAW’s from  $a$  to  $b$  at criticality:  $G_{n,L}(a, b) \propto |a - b|^{-2x_L(n)}$ . The natural generalization for the chiral case is that the  $L$  self-avoiding walks have no parallel self-contacts. Then the computation below of the transfer matrix at criticality ( $\mu = 1$ ) on finite strips shows that the chiral exponents  $\tilde{x}_L$  are identical to the nonchiral exponents  $x_{2L}$  for twice as many connectors. The nonchiral values  $x_L = (L^2 - 1)/12$  known from the Coulomb-gas technique<sup>10</sup> then determine all the  $\tilde{x}_L$ .

Now we connect the watermelon exponents to physical properties such as  $\gamma$  and  $\nu_\theta$ . First, the size exponent  $\nu_\theta = (2 - x_2)^{-1}$  is unchanged by the chirality constraint because it takes the same value for ring polymers as for linear polymers, and ring polymers are unaffected by the chirality constraint. The exponent  $\gamma$  is given by  $\nu_\theta(d - 2\tilde{x}_1) = \nu_\theta(d - 2x_2) = \frac{6}{7}$ . Note that the ring exponent  $\alpha$  is<sup>14</sup> also  $\frac{6}{7}$  so the two terms of (1.8) scale with the same power of  $N$ , as required for consistency.

The diffusion result  $\langle\langle R^2(N) \rangle\rangle \propto N$  might seem almost coincidental. However, it follows directly from the relationship  $\tilde{x}_1 = x_2$  between the chiral exponent with one leg and the nonchiral exponent with two legs:

$$\gamma + 2\nu_\theta - 1 = \frac{4 - 2x_2}{2 - x_2} - 1 = 1. \quad (2.4)$$

The “mysterious cancellation of exponents”<sup>12</sup> which yields diffusion in the percolation picture is relatively

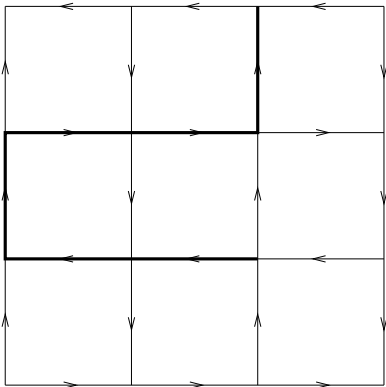


FIG. 2. A directed walk on the Manhattan lattice. Note that all allowed self-contacts on this lattice are antiparallel.

simple in the polymer picture, and does not depend on the specific value of  $x_2$ .

The result  $\tilde{x}_L = x_{2L}$  for chiral polymers is exactly the same as for polymers at  $\theta$  on the Manhattan directed lattice (Fig. 2), which by construction has no parallel self-contacts<sup>17</sup>. Hence we learn that the detailed structure of the Manhattan lattice is in some sense irrelevant: it is the short-ranged constraint of no parallel self-contacts which determines the universality class. Another piece of information about polymers follows from the beautiful result of Cardy<sup>18</sup> for the conductivity  $\sigma_{xx} = \frac{\sqrt{3}e^2}{4h}$  at the critical energy. This fixes the lattice diffusion constant through the Einstein relation<sup>11,12</sup>, and therefore predicts a value for the combination of prefactors in (2.2).

The chiral polymer model discussed here is just one point of a two-parameter family of models with antiparallel self-contacts weighted by some real number  $w$  and parallel self-contacts by some possibly different number  $v$ . Then  $w = v$  gives ordinary two-dimensional self-interacting polymers, while  $v = 0$  gives the chiral polymer ensemble. One expects a “coiled” polymer phase for  $w = 0$  and  $v \rightarrow \infty$ , different from the conventional collapsed polymer phase. The full phase diagram of these models in the  $(w, v)$  plane is a rich subject; the corresponding problem defined in terms of parallel and antiparallel self-contacts, rather than hexagons, has been investigated numerically on the square lattice<sup>19,20</sup>. A conformal field theory approach suggests the possibility of continuously varying  $\gamma$  between the chiral polymer and ordinary polymer  $\theta$ -points<sup>21</sup>. We remark in passing that the lattice  $\theta'$  model defined here in terms of hexagon weights  $(w, z)$  has a number of advantages for this problem: the critical point  $w = \frac{1}{2}$  is known exactly, and the exact relation discussed below between transfer matrices suggests that this model may be solvable by vertex methods.

The remainder of this section establishes the connection  $\tilde{x}_L = x_{2L}$  between the watermelon exponents of chiral polymers on the hexagonal lattice and those of nonchiral polymers, and can be skipped by nonspecialists. A powerful method to obtain properties of polymer models

is by using conformal invariance to analyze the results of finite-size transfer matrix calculations<sup>22,23</sup>. Since there are reviews of the technique<sup>23,24</sup>, some minor details will be omitted.

The goal will be to find the transfer matrix for  $L$  polymers on a cylinder of circumference  $h$  hexagons. The scaling dimensions  $\tilde{x}_L$  can be derived from the finite-size correlation length  $\xi_{L,h}$ , which is determined by the largest eigenvalue  $\lambda_{L,h}$  of the transfer matrix:

$$\xi_{L,h} = -\frac{1}{\log \lambda_{L,h}}. \quad (2.5)$$

The  $\tilde{x}_L$  are then estimated for successively larger cylinders using

$$\tilde{x}_{L,h} = -\left(\frac{2}{\sqrt{3}}\right) \frac{h}{2\pi} \log \lambda_{L,h}. \quad (2.6)$$

The geometrical factor  $\frac{2}{\sqrt{3}}$  comes from the hexagonal lattice dimensions and is 1 for a square lattice.

The transfer matrix acts on “configurations” of horizontal edges. A configuration consists of the state of all the horizontal edges, plus information on which oppositely directed edges are paired (originated from the same loop), plus information on which hexagons between horizontal edges have been passed on the left or right. The entries in the matrix sum over the different possible states of the vertical edges which can link two configurations. Each entry is weighted by a factor  $w$  for each hexagon passed on one side,  $v$  for each hexagon passed on both sides, and  $\mu$  for each edge. For the critical point of chiral polymers,  $w = \frac{1}{2}$ ,  $v = 0$ , and  $\mu = 1$ ; setting  $v = w = \frac{1}{2}$  gives the ordinary  $\theta$ -point, while taking  $w = v = 1$  and  $\mu = \mu_c = (2 + \sqrt{2})^{-1}$  gives the critical point of noninteracting SAWs.

Note that parallel self-contacts can only occur for one polymer in the cylindrical geometry when the polymer winds around the cylinder. As a result the surface critical exponents, which follow from the transfer matrix on the strip (closed boundary conditions) rather than on the cylinder (periodic boundary conditions), are unmodified from the nonchiral case. Upon conformal mapping from the cylinder back to the plane, polymers which wrap around the cylinder become polymers which wrap around the origin of the plane, and closed boundary conditions correspond to a branch cut which polymers cannot cross. The equivalence of surface exponents to those of the nonchiral  $\theta$ -point was previously obtained for the Manhattan lattice<sup>25</sup>.

Table I gives the estimated scaling dimensions  $\tilde{x}_1$  and  $\tilde{x}_2$  from cylinders of various sizes. The first few can be done by hand, while the larger matrices are done by computer. The leading eigenvalues are exactly the same as for those of twice as many nonchiral polymers. This connection is in retrospect not too surprising, since the condition of no parallel self-contacts for a polymer from  $A$  to  $B$  in the chiral case is exactly the condition that another

$h$	$\tilde{x}_{1,h} = x_{2,h}$	$x_{\text{extrap.}}$	$\tilde{x}_{2,h} = x_{4,h}$	$x_{\text{extrap.}}$
2	0.254768			
3	0.259127	0.23788		
4	0.256212	0.24859	1.52861	1.2814
5	0.254221	0.24911	1.39654	1.26398
6	0.253007		1.34308	1.25603
7	0.25224		1.31513	
8			1.2984	
$\infty$	$\frac{1}{4} = 0.25$		$\frac{5}{4} = 1.25$	

TABLE I. Results of transfer matrix calculations for one and two chiral polymers (identical to results for two and four nonchiral polymers), on cylinders of circumference  $h$  hexagons. The largest eigenvalue of the transfer matrix is related to  $x_{L,h}$  through (2.6). The convergence to the predicted values  $\tilde{x}_1 = \frac{1}{4}$  and  $\tilde{x}_2 = \frac{5}{4}$  is seen to be quite rapid. The extrapolated values are obtained by using three consecutive values of  $x_h$  to fix the constants in  $x_h = c_1 + c_2 h^{-c_3}$ , then taking  $c_1$  as an estimate of  $x_\infty$ .

polymer can be added from  $A$  to  $B$  in the nonchiral case. The subleading eigenvalues can differ, however, so there may not be a simple equivalence between states of  $L$  chiral polymers and  $2L$  nonchiral polymers. The critical properties of the nonchiral model follow from Coulomb gas results for the  $O(n)$  model<sup>10</sup>, so we have

$$x_L = \frac{L^2 - 1}{12}, \quad \tilde{x}_L = \frac{4L^2 - 1}{12}. \quad (2.7)$$

The chiral exponents  $\tilde{x}_L$  are the same as those of the  $\theta$ -point on the Manhattan lattice<sup>26</sup>. There are Monte Carlo results for another hexagonal lattice model believed to lie in the Manhattan universality class, the ‘‘smart kinetic growth SAW’’<sup>27</sup>, which are consistent with the above values.

### III. THE CLASSICAL LOCALIZATION EXPONENT

When the particle energy  $E$  moves away from the critical energy, the trajectories become less extended and the mean distance from the origin after  $N$  time steps is reduced. In this section, we take the lattice disorder average in order to express  $P(a, b, N)$ , the probability that after  $N$  steps the particle has moved from  $a$  to  $b$ , as a weighted sum over linear and ring polymers. Simple properties of the weight function then yield an inequality connecting the localization exponent  $\nu$  to polymer exponents  $\gamma$  and  $\nu_\theta$ .

As in the preceding section, we fix an open or closed curve on the lattice and ask what fraction of potential realizations make this curve the correct trajectory.

The particle energy  $E$  is also varied in order to find the energy-integrated diffusion constant, and hence  $\nu$ . The weight of a curve is determined by the numbers of hexagons touched by the curve to the left and right: the requirement for a path to be the correct trajectory is that all the hexagons to the right lie above the particle energy. The probability that a path is the particle trajectory is a function of the number of different hexagons visited by the path. The requirement is that all the hexagons to the immediate left have energies larger than the particle energy, while those to the immediate right have energies smaller than the particle energy. The  $H_L$  hexagons on the left must have higher energies than the  $H_R$  on the right, which is true for  $\binom{H_L + H_R}{H_L}^{-1}$  of potentials. Furthermore, the particle energy must lie in the window of width  $\sim (H_L + H_R)^{-1}$  between the lowest potential on the left and the highest potential on the right. So the weight of an allowed path  $P_{AB}$  is

$$W(P_{AB}) \propto \frac{1}{(H_L + H_R) \binom{H_L + H_R}{H_L}} \approx \frac{H_L! H_R!}{(H_L + H_R + 1)!}. \quad (3.1)$$

The same result is obtained by integrating the probability  $\left(\frac{1+E}{2}\right)^{H_L} \left(\frac{1-E}{2}\right)^{H_R}$  over particle energy  $E$  to obtain a beta function.

Now we can again connect the expression (1.8) and the weight (3.1) to known properties of polymers. For fixed  $H = H_L + H_R$ , the weight is minimized if  $H_L = H_R$ , and using Stirling’s approximation is then  $W(H) \approx \frac{\sqrt{2\pi}}{2^H H^{1/2}}$ . The probability to get from  $a$  to  $b$  after  $N$  steps thus satisfies

$$P(a, b, N) \geq \sum_{\substack{\text{SAPs through } a \text{ and } b, \\ l = \text{length of SAP,} \\ q = \text{steps from } a \text{ to } b}} \frac{\delta_{N \bmod l, q}}{2^H H^{1/2}} + \sum_{\substack{\text{SAWs of length } N \\ \text{from } a \text{ to } b \\ \text{no || self-contacts}}} \frac{1}{2^H H^{1/2}}, \quad (3.2)$$

up to a possible numerical constant. The typical number of hexagons  $H$  scales linearly in  $N$  to sufficient accuracy that  $H^{1/2}$  can be replaced by  $N^{1/2}$  (this is verified numerically by Monte Carlo simulations, and if false would require an unexpected multifractality at the  $\theta$ -point). Summing over final positions  $b$  to find the mean squared displacement then gives

$$\langle\langle R^2(N) \rangle\rangle \geq N^{\gamma - 1 + 2\nu_\theta - \frac{1}{2}}. \quad (3.3)$$

Then from equation (1.7) we obtain an inequality connecting the localization exponent  $\nu$  for the plateau transition to polymer exponents  $\nu_\theta$  and  $\gamma$ :

$$1 - \frac{1}{2\nu} \geq \gamma + 2\nu_\theta - \frac{3}{2}. \quad (3.4)$$

For the chiral polymer model, the resulting prediction is  $\nu \geq 1$ , which is satisfied by the actual value  $\nu = \frac{4}{3}$ .

The usual nonchiral polymer exponents at  $\theta$  would predict  $\nu \geq \frac{7}{3}$  (cf. section IV), so again it is seen that the chirality constraint is essential. The fact that the lower bound is not reached shows that even in the limit of long paths, the number of hexagons to the left and right of the path cannot be assumed equal in calculating the weight (3.1). At the critical energy (section II), hexagons to the left and right contribute equally and this difference is irrelevant, but away from the critical energy the difference affects the scaling.

The exact value  $\nu = \frac{4}{3}$  is derived in the percolation picture<sup>4</sup> from the equivalence of closed trajectories at energy  $E$  to percolation hulls with  $p - p_c \propto E - E_0$ , where  $p_c$  is the critical probability for percolation and  $E_0$  is the critical energy. Such percolation hulls<sup>28</sup> have average size  $\xi \sim (p - p_c)^{-\frac{4}{3}}$ . We remark in passing that the value  $\nu = \frac{4}{3}$  can be understood in the polymer context from the fact the crossover exponent of the tricritical  $\theta$ -point is  $\phi = \frac{3}{7}$  (this value was first obtained using the connection to percolation<sup>14</sup>): then  $N^{-\phi} \sim (p - p_c)$  and  $\xi \sim (p - p_c)^{-\nu\phi/\phi} = (p - p_c)^{-\frac{4}{3}}$ . The reasons for stressing the inequality (3.4) here rather than the exact result are that the inequality follows immediately from the classical path weight on polymers and can be used to gain information on higher moments (Section IV).

The main result of this section is that the exact path weight induced by averaging over disorder and particle energy can be calculated for the classical lattice model. This weight yields the inequality (3.4) connecting statistics of chiral polymers to the critical exponent  $\nu$  of the classical plateau transition. The focus of the next section will be whether a similar relationship to polymers exists for the quantum plateau transition.

#### IV. HIGHER MOMENTS AND THE QUANTUM TRANSITION

The quantum Hall plateau transition shows several qualitative similarities with the semiclassical limit studied in the preceding sections of this paper. Both the quantum transition and the semiclassical limit have power-law delocalization at the critical energy and a finite critical conductivity. However, the quantum transition has proved much more difficult to describe theoretically, and remains a major open problem. A natural question is whether any generalization of the polymer mapping developed for the classical limit would serve as a useful approach for the quantum case. The goal of this section is to show that the diffusive behavior usually assumed to exist up to the localization length in the quantum case would be inconsistent with almost any such generalization, and present a numerical method and preliminary results to verify this assumption. We focus on one generalization in particular (to *nonchiral* polymers at  $\theta$ , for reasons described below) for conciseness.

The scaling laws of moments of the particle distribution function

$$\langle R^{2n}(t) \rangle \sim t^{\alpha(n)} \quad (4.1)$$

demonstrate an essential difference between the classical limit and the conventional picture of the quantum case. In this section  $\langle \rangle$  indicates averaging over particle energy and random potentials, while  $\langle \rangle_E$  indicates averaging over random potentials at fixed particle energy  $E$ . If particle motion is essentially diffusive on short length scales in the quantum case, then higher scaling laws beyond  $n = 1$  in (4.1) do not contain additional information. As discussed in the previous section, the mean squared displacement  $\langle R^{2n}(t) \rangle \sim t^{1-\frac{1}{2\nu}}$  contains the localization exponent  $\nu$ . This formula was obtained from the assumption that  $\langle R^2(t) \rangle_E$  increases linearly in time at each energy until the localization length is reached ( $R^2 \approx \xi(E)^2$ ), then saturates.

If the particle motion is truly diffusive up to the localization length, then  $\langle R^{2n}(t) \rangle_E \sim t^n$  until the localization length is reached, and

$$\langle R^{2n}(t) \rangle \sim t^{n-\frac{1}{2\nu}}, \quad (4.2)$$

with the localization length exponent  $\nu \approx 2.35 \pm 0.05^6$ . So if motion in the quantum case is diffusive up to the localization length, there are no nontrivial exponents to be found in higher moments of the particle displacement.

Higher moments in the *classical* case show nontrivial scaling, and consequently highly extended trajectories are much more common in the classical case than the quantum case, even though the localization length diverges more rapidly near  $E_c$  for the quantum case. For walks at the critical energy, it follows from the results of Section II that

$$\langle R^{2n}(t) \rangle_{E_c} \sim t^{2n\nu_\theta + \gamma - 1} = t^{(8n-1)/7}. \quad (4.3)$$

Hence, although the mean square displacement does increase linearly with time, higher moments have nontrivial power laws because the particle trajectories are not random walks but instead have “memory,” as required for the absence of self-intersections. The higher moments are more extended than they would be for simple diffusive motion (random walks).

A similar result holds for the classical case even when the average is extended to include the particle energy. The inequality (3.4) derived in Section III between polymer exponents at the chiral  $\theta$ -point and the scaling of the second moment  $\alpha(1) = 1 - \frac{1}{2\nu}$  from (4.1):

$$1 - \frac{1}{2\nu} \geq 2\nu_\theta + \gamma - \frac{3}{2} = \frac{1}{2}. \quad (4.4)$$

For the classical transition with  $\nu = \frac{4}{3}$ , the left side is  $\frac{5}{8}$  and the inequality is satisfied. Similarly for higher moments  $\langle R^{2n}(t) \rangle \sim t^{\alpha_c(n)}$

$$\alpha_c(n) \geq 2n\nu_\theta + \gamma - \frac{3}{2} = \frac{1}{2} + \frac{8(n-1)}{7}. \quad (4.5)$$

Hence for sufficiently large  $n$  the classical scaling exponents  $\alpha_c(n)$  are larger than the quantum exponents  $\alpha(n) = n - \frac{1}{2\nu}$ , if the motion in the quantum case is indeed diffusive.

In the remainder of this section, we consider the question of how quantum interference keeps the quantum case from being related to a polymer ensemble in the same way as the classical case. One polymer ensemble in particular is attractive for the quantum case because the ensemble is similar to the classical one and the value  $\nu = \frac{7}{3}$  appears in this ensemble, but this connection predicts nondiffusive motion up to the localization length. Monte Carlo numerics are used to test the assumption of diffusive motion in the quantum case; if verified this assumption would rule out a simple connection to polymers.

The approach of the previous section was to generate a positive weight on electron paths by averaging over disorder with the electron path held constant. In lattice models for the quantum transition, it should be possible to attribute a positive weight to each path on the lattice, and then these weights may be connected to some polymer problem, presumably different from the chiral ensemble discussed above for the classical limit. The first statement (that there is an assignment of weights) is somewhat trivial from a mathematical point of view: there are many paths on the lattice between any pair of points, and hence given any positive probabilities to reach different points on the lattice after  $N$  steps, there is some assignment of positive path weights which results in the given probabilities. The difficult question is whether there is an assignment of weights which is physically meaningful and related to some local two-dimensional theory, as in the classical case. The next paragraphs define a real (not necessarily positive) path weight; this weight is positive in the absence of interference, and the leading interference contribution to this path weight from “cooperons” vanishes, though higher contributions do not.

For fixed disorder, different paths  $W_{AB}^i$  from  $A$  to  $B$  contribute to the amplitude, and the probability  $P_{AB}$  to get from  $A$  to  $B$  includes both diagonal terms  $|W_{AB}^i|^2$  and cross terms. Here and in the following we assume a discretized model for the quantum case, similar to the lattice model introduced previously for the classical limit. We start by considering two paths which do not cross: then the disorder average generates a random phase which cancels the cross terms, leaving only the (positive) diagonal terms. The remaining question is what occurs for intersecting paths; this is known to be the case of interest for the quantum effects causing weak localization.

If the cross terms did vanish, then in the discretized model where  $\lambda_D$  is effectively zero,  $P_{AB}$  would be a sum over (not necessarily self-avoiding) paths with some positive weight, the “quantum path weight” (QPW). A real weight can be defined even if cross terms are present by adding to the direct contribution of each path half of all

its disorder-averaged cross terms with other paths. The QPW picture can break down if, for energies near the critical energy, the cross terms become large enough to drive the weight negative for long paths. However, the leading interference corrections vanish upon disorder averaging, and a finite strength of interference is required to drive the path weight negative, so it is seemingly possible that a positive QPW exists for the paths near the critical energy which determine  $\nu$ . This motivates the conjecture, tested in the remainder of this section, that the universal large-length-scale properties of the plateau transition may be related to those of some classical generalized polymer model (i.e., a sum over paths with positive weights), in similar fashion to the relationships found in sections II and III between the classical percolation limit and the chiral polymer model.

The remaining step is to determine whether any universality class of classical polymers can reproduce the weights which follow from disorder averaging in the quantum case. It seems worthwhile to identify possibilities, since exact results have been obtained for many two-dimensional polymer models by Coulomb gas and CFT techniques. The QPW should give nearly the classical weight (3.1) to paths which are classically allowed or include a small number of quantum tunneling events, but should not allow of order  $N$  tunneling events for an  $N$ -step path since then the motion is simply diffusive even away from the critical energy. A speculative possibility for the quantum transition is the *nonchiral* polymer ensemble at  $\theta$ . The expectation that quantum mechanics should allow some unfavorable steps (but fewer than  $\sim N$ ) matches the fact that a typical polymer in the nonchiral ensemble has some parallel self-contacts, but fewer than of order  $N$ . A simple argument that the number of parallel self-contacts is subextensive ( $< N$ ) is that a ring polymer has no parallel self-contacts, so that parallel self-contacts are in some sense a boundary property.

A surprise is that the value  $\nu = \frac{7}{3}$  (which has attracted attention as the simplest rational consistent with numerics) appears from exponents of the nonchiral ensemble. The inequality (3.4) connecting the localization exponent  $\nu$  to nonchiral polymer exponents predicts, since  $\gamma = \frac{8}{7}$ ,

$$1 - \frac{1}{2\nu} \geq \gamma + 2\nu_\theta - \frac{3}{2} = \frac{11}{14}, \quad (4.6)$$

or  $\nu \geq \frac{7}{3}$ . Hence the value  $\frac{7}{3}$  appears in the critical properties of a polymer ensemble closely related to the polymer ensemble describing the classical plateau transition. The lower bound is realized if paths have asymptotically the same number of hexagons to the left as to the right ( $H_R \sim H_L$ ), which should be a better approximation for the less convoluted paths in the quantum case. As seen below, however, this inequality predicts scaling laws for higher moments which appear to be ruled out numerically in the quantum case. Hence quantum interference seems to be relevant at the quantum transition even beyond the level of changing path weights.



We note in passing that the desired property of diffusion at the critical energy does not have any simple interpretation as a statement about the polymer ensemble, since it is only after integrating over particle energy that the polymer weights may appear. This situation is familiar from the Liouvillian approach to the transition<sup>16,31</sup>, where the transition is mapped onto a different problem which contains the exponent  $\nu$  but not the critical conductivity. Note that the previous appearance of the value  $\frac{7}{3}$  in a semiclassical average over a single percolation trajectory<sup>29</sup> does not clearly relate to a critical point, when the electron is delocalized over multiple trajectories. Now we discuss how numerics can test whether the appearance of this value in this polymer ensemble is just a numerical coincidence.

There are numerically testable consequences which can be used to check whether nonchiral polymers at  $\theta$  are indeed related to the quantum case. The polymer problem predicts various moments of the disorder- and energy-averaged displacement: it was shown in the previous paragraph that the mean squared displacement  $\langle R^2(N) \rangle \sim N^{11/14}$ , so that  $\nu = \frac{7}{3}$ . Similar predictions follow for higher moments, such as  $\langle R^4(N) \rangle \sim N^{4\nu+\gamma-3/2} = N^{27/14}$ , or  $\alpha(2) = \frac{27}{14}$ . This can be compared to the null hypothesis of diffusion up to the localization length, which predicts  $\langle R^4(N) \rangle \sim N^1$ .<sup>78</sup>

We have performed Monte Carlo simulations with up to 1800 states in the lowest Landau level to track the evolution of a localized wave packet in a disordered potential (the method is similar to that of<sup>30</sup>). The error bars are larger for the fourth moment than for the second because finite-size effects are more pronounced on the extended paths which dominate the fourth moment, but it appears that  $\alpha(2) = 1.8 \pm 0.1$ , which if correct is sufficient to rule out  $\alpha(2) = 27/14 \approx 1.92$ . With larger system sizes, it should be straightforward to confirm the assumption of diffusive motion up to the localization length. Then a polymer description would have to have  $\nu = 1/2$  (either dense polymers or random walks), but no appropriate ensemble is obvious. It seems more likely that strong quantum interference prevents a physically meaningful assignment of path weights in the quantum case.

To summarize, this section discussed differences between the classical and quantum transitions which become apparent in higher moments of the particle distribution function. Numerics seem to support the picture of diffusion up to the localization length and rule out the simplest polymer model for the quantum case. In closing, we mention briefly connections between the polymer models discussed in this paper and conformal field theory (CFT) approaches to the transition. The low-temperature  $O(n)$  phase also appears in a large- $N$  expansion of the disorder-averaged Liouvillian theory, which is similar to a partially supersymmetric complex  $O(N)$  model, with  $N \rightarrow 1$  the physical limit<sup>31</sup>. Recent work<sup>32,33</sup> on the critical point of Dirac fermions in a non-abelian random vector potential found a  $c = -2$  dense

polymer problem hidden in the critical theory for several different types of disorder. Since upon adding additional disorder (random mass and chemical potential) the abelian version of this critical point flows to the plateau transition fixed point<sup>34</sup>, the appearance of polymer subalgebras may be generic to this class of random critical points.

The author wishes to thank H. Saleur and S. Girvin for helpful suggestions.

- 
- <sup>1</sup> R. B. Laughlin, Phys. Rev. B **23**, 5632 (1981).
  - <sup>2</sup> A. M. M. Pruisken, Nucl. Phys. B **235**, 227 (1984).
  - <sup>3</sup> M. Zirnbauer, J. Math. Phys. **38**, 2007 (1997).
  - <sup>4</sup> S. Trugman, Phys. Rev. B **27**, 7539 (1983).
  - <sup>5</sup> I. A. Gruzberg, A. W. W. Ludwig, and N. Read, Phys. Rev. Lett. **82**, 4524 (1999).
  - <sup>6</sup> B. Huckestein, Rev. Mod. Phys. **67**, 357 (1995).
  - <sup>7</sup> J. T. Chalker and P. D. Coddington, J. Phys. C **21**, 2665 (1988).
  - <sup>8</sup> S. Das Sarma, in *Perspectives in Quantum Hall Effects*, ed. S. Das Sarma and A. Pinczuk (Wiley, New York, 1997).
  - <sup>9</sup> P. G. de Gennes, Phys. Lett. **A38**, 339 (1972).
  - <sup>10</sup> B. Nienhuis, Phys. Rev. Lett. **49**, 1063 (1982); B. Nienhuis, in *Phase Transitions and Critical Phenomena*, ed. C. Domb and J. L. Lebowitz (Academic, London, 1986), vol. 11.
  - <sup>11</sup> F. Evers, Phys. Rev. E **55**, 2321 (1997).
  - <sup>12</sup> V. Gurarie and A. Zee, Int. J. Mod. Phys. B **15**, 1225 (2001).
  - <sup>13</sup> A. Coniglio *et al.*, Phys. Rev. B **35**, 3617 (1987).
  - <sup>14</sup> B. Duplantier and H. Saleur, Phys. Rev. Lett. **59**, 539 (1987).
  - <sup>15</sup> H. P. Wei, D. C. Tsui, M. A. Paalanen and A. M. M. Pruisken, Phys. Rev. Lett. **61**, 1294 (1988); H. P. Wei, S. Y. Lin, D. C. Tsui, and A. M. M. Pruisken, Phys. Rev. B **45**, 3926 (1992).
  - <sup>16</sup> J. Sinova, V. Meden, and S. M. Girvin, Phys. Rev. B **62**, 2008 (2000).
  - <sup>17</sup> R. M. Bradley, Phys. Rev. A **41**, 914 (1990).
  - <sup>18</sup> J. Cardy, Phys. Rev. Lett. **84**, 3507 (2000).
  - <sup>19</sup> A. Trovato and F. Seno, Phys. Rev. E **56**, 131 (1997).
  - <sup>20</sup> T. Prellberg and B. Drossel, Phys. Rev. E **57**, 2045 (1998).
  - <sup>21</sup> J. L. Cardy, Nucl. Phys. B **419**, 411 (1994).
  - <sup>22</sup> B. Derrida, J. Phys. A **14**, L5 (1981).
  - <sup>23</sup> H. Saleur, J. Phys. A **20**, 455 (1987).
  - <sup>24</sup> C. Vanderzande, *Lattice Models of Polymers* (Cambridge, 1998).
  - <sup>25</sup> S. L. M. de Queiroz and J. M. Yeomans, J. Phys. A **24**, L933 (1991).
  - <sup>26</sup> T. Prellberg and A. Owczarek, J. Phys. A **27**, 1811 (1994).
  - <sup>27</sup> D. Bennett-Wood, A. L. Owczarek, and T. Prellberg, Physica A **206**, 283 (1994).
  - <sup>28</sup> M. den Nijs, J. Phys. A **12**, 1857 (1979).
  - <sup>29</sup> G. V. Mil'nikov and I. M. Sokolov, JETP Lett. **48**, 536 (1988).

- <sup>30</sup> S. Boldyrev and V. Gurarie, `cond-mat/0009203` (2000).
- <sup>31</sup> J. E. Moore, A. Zee, and J. Sinova, *Phys. Rev. Lett.* **87**, 8704-8707 (2001).
- <sup>32</sup> A. LeClair, `cond-mat/0011413` (2000).
- <sup>33</sup> M. J. Bhaseen, J.-S. Caux, I. I. Kogan, and A. M. Tsvelik, `cond-mat/00012240` (2000).
- <sup>34</sup> A. W. W. Ludwig, M. P. A. Fisher, R. Shankar, and G. Grinstein, *Phys. Rev. B* **50** 7526 (1994).